

Investigating the role of calcium and biological trace elements in hypericin photodynamic therapy induced tumor cell death using nuclear microscopy

P.S.P. Thong ^{a,*}, F. Watt ^b, M.Q. Ren ^b, K.C. Soo ^a, M. Olivo ^a

^a Division of Medical Sciences, National Cancer Centre, 11 Hospital Drive, Singapore 169610, Singapore

^b Centre for Ion Beam Applications, National University of Singapore, Singapore

Available online 23 March 2005

Abstract

Photodynamic therapy (PDT) is a promising new modality for the treatment of several types of cancer, including nasopharyngeal carcinoma (NPC). It involves the use of a photosensitising drug together with exposure to light to kill tumor cells via the generation of reactive oxygen species (ROS). Since transition trace metal ions such as iron are required in the generation of ROS in biological systems, it is possible that they also play a role in PDT-induced cell death. Additionally, some studies also show the involvement of calcium in PDT-induced apoptosis. Thus both major and trace biological elements may be involved in PDT cell killing mechanisms.

This study involves the analysis of human NPC xenograft tumors in murine models using the National University of Singapore nuclear microscope. PDT was carried out using the photosensitizer hypericin under various conditions. The microbeam techniques of particle induced X-ray emission, Rutherford backscattering spectrometry and scanning transmission ion microscopy were used to quantify elemental concentrations in cryo-fixed sections of tumor tissue. Preliminary results are presented as well as their implications for the mechanisms underlying photodynamic cell killing.

© 2005 Elsevier B.V. All rights reserved.

PACS: 87.64; 87.15.M; 07.85.F

Keywords: PDT; Hypericin; Tumor death; Calcium; Trace elements

1. Introduction

Photodynamic therapy (PDT) is a promising new modality for the treatment of several types of cancer, including nasopharyngeal carcinoma

* Corresponding author. Tel.: +65 63266192; fax: +65 63720161.

E-mail address: nmstsp@nccs.com.sg (P.S.P. Thong).

(NPC). It involves the use of a photosensitising drug together with exposure to light of a specific wavelength to kill tumor cells via the generation of reactive oxygen species (ROS) [1]. Advantages of PDT over other therapies include low toxicity of the drug used, tumor selectivity, localised treatment and little or manageable side effects [2].

Since PDT works via ROS generation and transition trace metal ions such as Fe are required in the generation of ROS in biological systems [3], it might also be possible that trace metal ions play a role in PDT-induced cell death. Additionally, some studies also show the involvement of Ca in PDT-induced apoptosis [4,5]. Thus both major and trace biological elements may be involved in PDT cell killing mechanisms.

This study involves nuclear microscopic analysis of human NPC xenograft tumors in murine models subjected to PDT using hypericin, a photosensitiser extracted from plants commonly known as St John's wort. Hypericin has shown great promise as a photosensitiser for PDT, and has been shown to induce both apoptotic and necrotic cell death [6].

The outcome of PDT depends on conditions used during the therapy. Parameters which affect PDT outcome include the drug and light doses, the light fluence rate and the time between drug administration and exposure to light, or the drug-light interval [7–10]. With a short drug-light interval, the high concentration of drug in circulation results in indirect cell kill via “vascular” mechanisms, in which the vasculature surrounding the tumor is destroyed, leading to hypoxia and tumor death [9]. With a longer drug-light interval, the drug accumulates in the tumor, resulting in direct photo-destruction of the tumor [10].

The nuclear microscope facility at the National University of Singapore is particularly suited for elemental analysis of biological specimens [11,12]. Using a 2.1 MeV proton beam focused to a 2 μm spot size, the complementary techniques, Rutherford backscattering spectrometry (RBS), particle induced X-ray emission (PIXE) and off-axis scanning transmission ion microscopy (STIM), were carried out in the analysis of tumor tissue sections from mice subjected to hypericin-PDT as well as from mice not subjected to PDT.

2. Materials and methods

2.1. Human NPC cell line and murine models

The cell line used, NPC/HK1, was established from well-differentiated NPC, and was kindly provided by Prof. K.M. Hui of the National Cancer Centre, Singapore. A cell suspension of 1.5×10^6 HK1 cells per 100 μl was prepared in phosphate buffered saline (PBS) and a volume of 100 μl was injected sub-cutaneously into each flank of 6–8-week-old male Balb/c nude mice. The mice were kept for 10–14 days for the tumors to grow to sizes between 100 and 300 mm^3 . The tumor volume was estimated by measuring the tumor dimensions in three orthogonal directions (d_1, d_2, d_3) and using the formula, volume = $(\pi/6 \times d_1 \times d_2 \times d_3)$.

2.2. Photosensitiser preparation and administration

Five mg/ml stock solutions of hypericin (Molecular Probes, Inc., Eugene, OR, USA) were prepared in dimethyl sulfoxide (DMSO) and stored in the dark at -20°C . Prior to PDT, the stock solution was freshly diluted in DMSO and PBS and injected intravenously into the tail veins of the mice at doses of 5 mg/kg body weight (except 2 mg/kg in one sample). The animals were then kept in minimal lighting for the duration of the drug-light interval.

2.3. Photodynamic therapy

To carry out hypericin-PDT, we fitted a broadband halogen light source (Zeiss KL1500 light unit) with a customised band-pass filter for the wavelength range 560–640 nm, suitable for the absorption peak of 590 nm for hypericin. The output light intensity was adjusted to give a light fluence rate of 25 mW/cm^2 , measured using a power meter (Coherent, USA). After a drug-light interval of either 1 h (1h-PDT) or 6 h (6h-PDT), the PDT tumors were exposed to a light dose of 30 J/cm^2 with the animals under light anaesthesia. Dark control tumors on the contra-lateral sides were not exposed to light.

2.4. Sample preparation

After PDT, the animals were kept in the dark prior to sacrifice by carbon dioxide at 24 h post-PDT. The tumors were then excised and cryo-fixed. Cryo-fixation was carried out in liquid nitrogen-cooled isopentane to snap freeze the tumors placed in embedding material in cups shaped from aluminium foil. The frozen tissue blocks were cut in a cryostat operating at -20°C . Sections were cut at $20\ \mu\text{m}$, picked up on freshly prepared sub-micron pioloform film and freeze-dried prior to analysis using the nuclear microscope in the Centre for Ion Beam Applications, National University of Singapore (NUS). Adjacent sections were cut for corresponding haematoxylin and eosin staining. Tumor tissue from mice which were not subjected to PDT were likewise processed.

2.5. Nuclear microscopy

The NUS nuclear microscope was set to operate on a 2.1 MeV proton beam focussed to approximately $2\ \mu\text{m}$ beam spot. Off-axis scanning transmission ion microscopy (STIM) was used for sample imaging, Rutherford backscattering spectrometry (RBS) for characterisation of C, N and O for sample density and charge normalisation. Particle induced X-ray emission (PIXE) was used in conjunction with RBS for quantitative analysis of major and trace elements. PIXE was carried out using a Si(Li) detector fitted with a customised $300\ \mu\text{m}$ Perspex “magic” filter. Bulk analysis of the samples was carried out by raster-scanning the beam over large areas (up to $4\ \text{mm} \times 4\ \text{mm}$) of

the tissue sections. Within areas of interest, higher resolution scans were carried out, from which individual cells were marked out for single cell analyses using the OM_DAQ data acquisition software [13].

3. Results

3.1. Bulk analysis of tumor sections

Table 1 shows the average concentrations (ppm) of major and trace biological elements (standard errors in parentheses) in (a) tumors subjected to 1h-PDT, (b) dark control tumors from 1h-PDT mice, (c) tumors subjected to 6h-PDT and (d) tumors from mice which were not subjected to PDT.

The results show a decrease of P and K in both 1h-PDT and 6h-PDT tumors compared to non-PDT tumors and an increase in Ca in 1h-PDT tumors compared to non-PDT tumors but not in 6h-PDT tumors. There is also an unexpected increase in Ca in dark control tumors in mice subjected to 1h-PDT on the contra-lateral side. There were no significant changes in the concentrations of the trace elements Fe and Zn. However, there appears to be an increase in Cu, although data with better statistics has to be collected to confirm this.

3.2. Analysis of single cells within tumor sections

Within the high-Ca areas in the 1h-PDT tumor, higher resolution scans were carried out. Fig. 1 shows the PIXE elemental maps from a

Table 1

Average bulk concentrations (ppm, standard errors in parentheses) of biological elements in (a) tumors subjected to 1h-PDT, (b) dark control tumors from mice subjected to 1h-PDT, (c) tumors subjected to 6h-PDT and (d) tumors from mice which were not subjected to PDT

Element	(a) 1h-PDT ($n = 3$)	(b) 1h-dark ($n = 2$)	(c) 6h-PDT ($n = 3$)	(d) Non-PDT ($n = 5$)
P	7380 (3188)	9233 (2456)	7936 (1294)	14,501 (845)
S	6906 (585)	7984 (1813)	5886 (1456)	9129 (327)
Cl	9113 (1073)	3136 (860)	7428 (2784)	7414 (1074)
K	4188 (3139)	6786 (1990)	5517 (1432)	18,457 (1849)
Ca	1486 (486)	1020 (151)	582 (201)	557 (100)
Fe	165.1 (58.4)	90.5 (46.9)	113.3 (25.7)	107.4 (16.3)
Cu	22.4 (13.1)	17.2 (8.2)	19.3 (8.0)	7.4 (1.1)
Zn	89.4 (10.0)	98.7 (24.9)	77.3 (15.3)	95.8 (3.8)

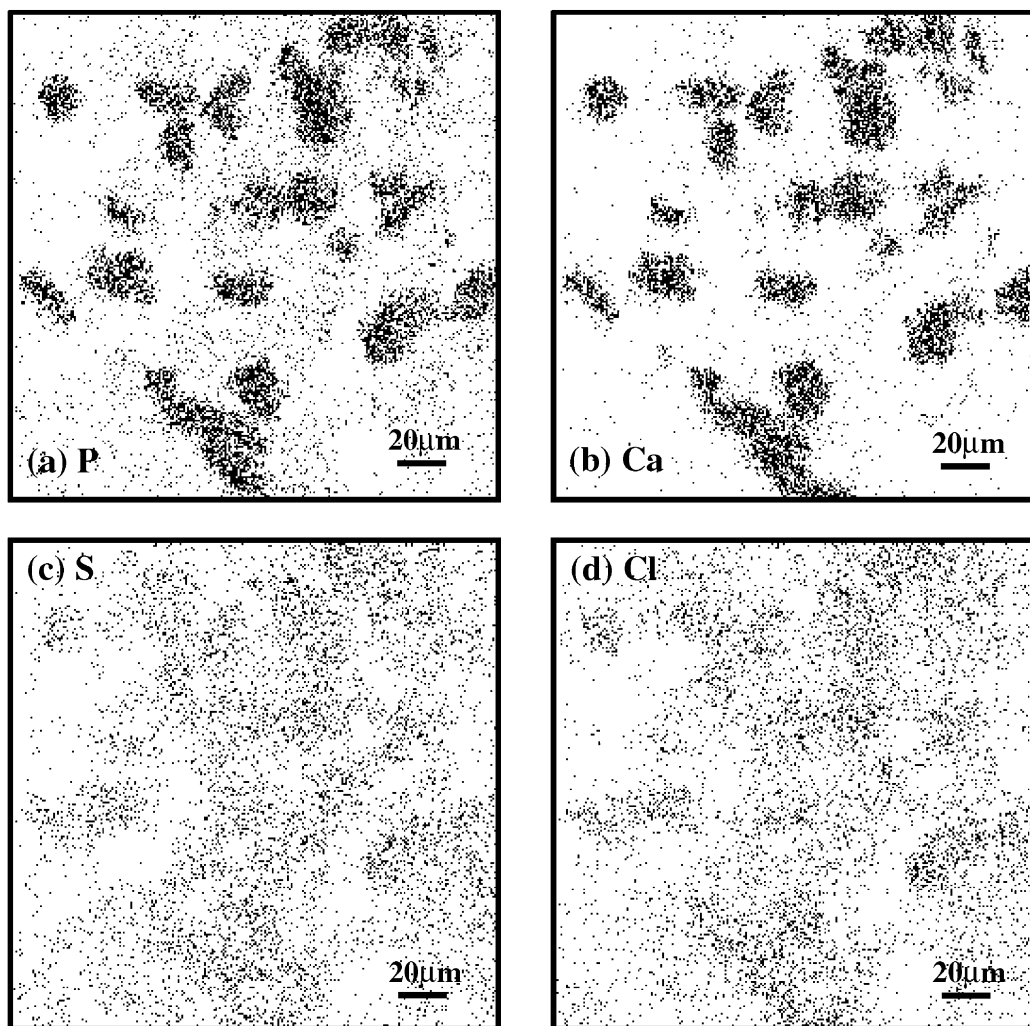


Fig. 1. PIXE elemental maps from a $200\ \mu\text{m} \times 200\ \mu\text{m}$ scan of a tumor sample subjected to hypericin-PDT after a 1 h drug-light interval. The maps, obtained using a 2.1 MeV proton beam focussed to approximately $2\ \mu\text{m}$ in diameter, show the distribution of (a) P, (b) Ca, (c) S and (d) Cl.

$200\ \mu\text{m} \times 200\ \mu\text{m}$ scan showing the distribution of (a) P, (b) Ca, (c) S and (d) Cl.

From the higher resolutions scans, a selection of high-Ca cells was marked for single cell analysis. Fig. 2 shows the average elemental concentrations (ppm) of (a) P and Ca, (b) S and Cl and (c) Fe and Zn in individual cells in a 1h-PDT tumor (solid bars ■) and the dark control tumor on the contra-lateral side (hollow bars □). The cells in the PDT tumor exhibit distinctly high levels of P, Cl

and Ca. The cells in the dark control tumor also exhibited high levels of Ca and P (albeit not as high as in the PDT tumors), but not Cl, unlike in the PDT tumor.

A higher level of Fe was seen in the dark control tumor compared to the PDT tumor while the Zn level was the same in both PDT and control tumors. The analysis of Cu concentrations in cells was not achieved with the current set-up due to the high amounts of Ca contributing to Ca pile-

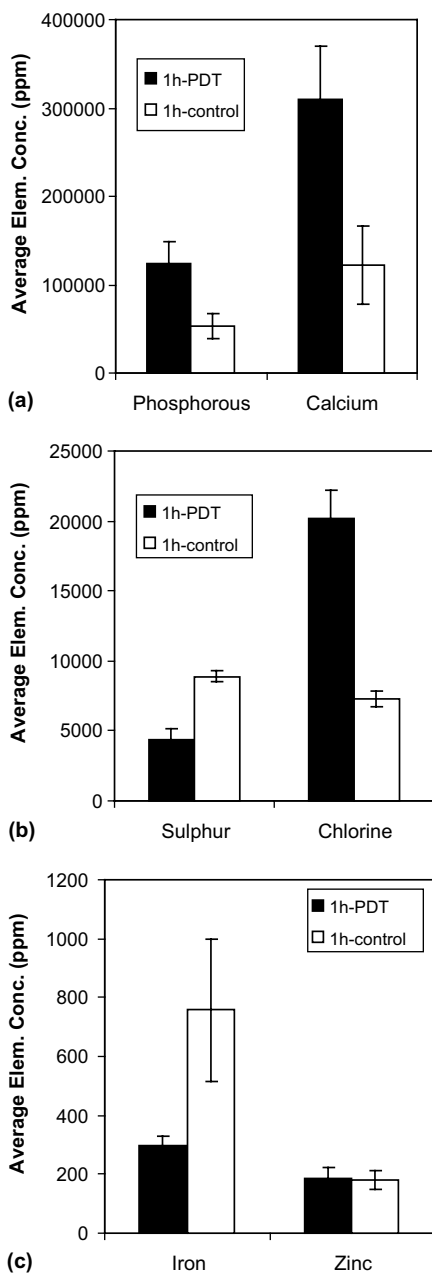


Fig. 2. Average elemental concentrations (ppm) of (a) P and Ca, (b) S and Cl and (c) Fe and Zn in single cells a 1h-PDT tumor (solid bars ■) and in the dark control tumor on the contra-lateral side (hollow bars □).

up peaks with energies close to those of the $\text{CuK}\alpha$ and $\text{K}\beta$ X-ray emission peaks.

4. Discussion

Bulk analysis of 1h-PDT tumors showed an increase in Ca levels compared to non-PDT tumors. This is in agreement with numerous reports that PDT results in an increase in intracellular Ca and inorganic phosphate as part of the mechanism of PDT-induced cell death [4,5,14,15]. Bulk analysis of 6h-PDT tumor did not show any significant changes in Ca concentrations. This difference in response between the 1h- and 6h-PDT tumors may be attributed to the different pathways of cell death elicited by PDT using a short drug-light interval, namely vascular-mediated damage, and PDT using longer intervals, namely direct photo-damage.

Analysis of high-Ca cells within 1h-PDT tumor tissue showed an increase in intracellular P and Cl in addition to Ca. While the increase in P and Ca can be attributed to intracellular mechanisms of cell death [4,5,14,15], it is unclear what role, if any, Cl plays in PDT-induced cell damage. These high levels of P, Cl and Ca were only observed in single cell analyses whereas in the bulk analyses of tumor sections, only a moderate increase in Ca was observed. This suggests that the photo-damage induced by 1h-PDT was a localised event, probably around microvasculature within the tumors.

A high level of intracellular P and Ca was also observed in the 1h-dark control tumor on the contra-lateral side, although the levels were not as high as those in PDT tumors. This “partial response” in tumors which were not exposed to light can possibly be attributed to a PDT-induced inflammation primed immune response against distant lesions of the same cancer [16]. Indeed, it was recently reported that under low fluence rate PDT (14 mW/cm^2), a sub-lethal light dose (48 J/cm^2) elicited a strong inflammatory response as evidenced by increased levels of interleukin-6 (IL-6) and macrophage inflammatory proteins 1 and 2 (MIP-1 and MIP-2) [8]. In our experiments, PDT was also carried out under conditions of a low fluence rate (25 mW/cm^2) and low light dose (30 J/cm^2). Hence a strong inflammation primed immune response acting on the contra-lateral dark control tumor is plausible.

5. Conclusion

Our preliminary results show that P and Ca play important roles in mechanisms of PDT-induced cell death, both in vascular damage as well as in PDT-induced inflammation primed immune response under low fluence rates and low light dose conditions.

There appears to be an increase in Cu levels between PDT and non-PDT tumors, although data with better statistics has to be collected to confirm this. If confirmed, it could imply the involvement of Cu-mediated generation of ROS in the process of PDT-induced cell death. Alternatively, since Cu is an important co-factor in angiogenesis [17], increased Cu levels may indicate an attempt by the tumor to regenerate blood vessels after damage by PDT. This latter explanation opens up the possibility of using Cu-chelators to enhance the efficacy of PDT by suppressing the regeneration of tumor vasculature after PDT.

It would be of interest to carry out further work to distinguish the involvement of biological elements between the different modes of cell death, apoptosis and necrosis, both of which can be induced by hypericin-photodynamic therapy.

Acknowledgments

The authors thank Ms. Vanaja T, Ms. Bhuvana R, Ms. Yee KKL and Mr. Kho KW (National Cancer Centre, Singapore) for contributing to this work.

References

- [1] D.E.J.G.J. Dolmans, D. Fukumura, R.K. Jain, *Nat. Rev. Cancer* 3 (5) (2003) 380.
- [2] M. Olivo, K.C. Soo, *SGH Proc.* 9 (3) (2001) 197.
- [3] J.M. Gutteridge, *Chem. Biol. Interact.* 91 (2–3) (1994) 133.
- [4] H. Tajiri, A. Hayakawa, Y. Matsumoto, I. Yokoyama, S. Yoshida, *Cancer Lett.* 128 (2) (1998) 205.
- [5] A. Ruck, K. Heckelmiller, R. Kaufmann, N. Grossman, E. Haseroth, N. Akgun, *Photochem. Photobiol.* 72 (2) (2000) 210.
- [6] S.M. Ali, M. Olivo, *Int. J. Oncol.* 22 (6) (2003) 1181.
- [7] A.R. Kamuhabwa, P.M. Agostinis, M.A. D'Hallewin, L. Baert, P.A. de Witte, *Photochem. Photobiol.* 74 (2) (2001) 126.
- [8] B.W. Henderson, S.O. Gollnick, J.W. Snyder, T.M. Busch, P.C. Kousis, R.T. Cheney, J. Morgan, *Cancer Res.* 64 (6) (2004) 2120.
- [9] B. Chen, T. Roskams, Y. Xu, P. Agostinis, P.A. de Witte, *Int. J. Cancer.* 98 (2) (2002) 284.
- [10] D.E.J.G.J. Dolmans, A. Kadambi, J.S. Hill, K.R. Flores, J.N. Gerber, J.P. Walker, I.H.M.B. Rinkes, R.K. Jain, D. Fukurama, *Cancer Res.* 62 (15) (2002) 4289.
- [11] F. Watt, I. Orlic, K.K. Loh, C.H. Sow, P. Thong, S.C. Liew, T. Osipowicz, T.F. Choo, S.M. Tang, *Nucl. Instr. and Meth. B* 85 (1–4) (1994) 708.
- [12] M.Q. Ren, P.S. Thong, J. Makjanic, D. Ponraj, F. Watt, *Biol. Trace Elem. Res.* 71–72 (1999) 65.
- [13] G.W. Grime, M. Dawson, *Nucl. Instr. and Meth. B* 89 (1–4) (1994) 223.
- [14] M. Nishiwaki, Y. Fujise, T.O. Yoshida, E. Matsuzawa, Y. Nishiwaki, *Br. J. Cancer* 80 (1–2) (1999) 133.
- [15] A. Viola, N.W. Lutz, C. Maroc, C. Chabannon, M. Julliard, P.J. Cozzone, *Int. J. Cancer* 85 (5) (2000) 733.
- [16] T.J. Dougherty, C.J. Gomer, B.W. Henderson, G. Jori, D. Kessel, M. Korbelik, J. Moan, Q. Peng, *J. Natl. Cancer Inst.* 90 (12) (1998) 889.
- [17] Q. Pan, C.G. Kleer, K.L. van Golen, J. Irani, K.M. Bottema, C. Bias, M. De Carvalho, E.A. Mesri, D.M. Robins, R.D. Dick, G.J. Brewer, S.D. Merajver, *Cancer Res.* 62 (17) (2002) 4854.